



HAL
open science

Hexagonal and rhombohedral polytypes in indium selenide films grown on c-plane sapphire

Lola de Brucker, Matthieu Moret, Bernard Gil, Wilfried Desrat

► **To cite this version:**

Lola de Brucker, Matthieu Moret, Bernard Gil, Wilfried Desrat. Hexagonal and rhombohedral polytypes in indium selenide films grown on c-plane sapphire. *AIP Advances*, 2022, 12 (5), pp.055308. 10.1063/5.0091675 . hal-03689421

HAL Id: hal-03689421

<https://hal.science/hal-03689421>

Submitted on 30 May 2023

HAL is a multi-disciplinary open access archive for the deposit and dissemination of scientific research documents, whether they are published or not. The documents may come from teaching and research institutions in France or abroad, or from public or private research centers.

L'archive ouverte pluridisciplinaire **HAL**, est destinée au dépôt et à la diffusion de documents scientifiques de niveau recherche, publiés ou non, émanant des établissements d'enseignement et de recherche français ou étrangers, des laboratoires publics ou privés.

RESEARCH ARTICLE | MAY 05 2022

Hexagonal and rhombohedral polytypes in indium selenide films grown on c-plane sapphire

L. de Brucker; M. Moret; B. Gil; ... et. al



AIP Advances 12, 055308 (2022)

<https://doi.org/10.1063/5.0091675>View
OnlineExport
Citation

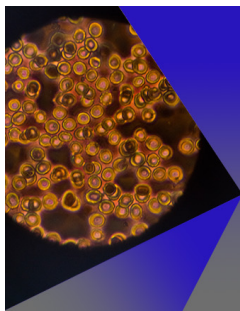
CrossMark

Articles You May Be Interested In

Further Studies of Polytypism in Lead Iodide

Journal of Applied Physics (November 2003)Polytypic phase formation in DyAl₃ by rapid solidification*Appl. Phys. Lett.* (January 1991)

Phase selective growth and properties of rhombohedral and cubic indium oxide

Appl. Phys. Lett. (July 2006)

AIP Advances

Special Topic: Medical Applications of Nanoscience and Nanotechnology

Submit Today!

Hexagonal and rhombohedral polytypes in indium selenide films grown on c-plane sapphire

Cite as: AIP Advances 12, 055308 (2022); doi: 10.1063/5.0091675

Submitted: 5 April 2022 • Accepted: 19 April 2022 •

Published Online: 5 May 2022



View Online



Export Citation



CrossMark

L. de Brucker, M. Moret,  B. Gil,  and W. Desrat^{a)} 

AFFILIATIONS

Laboratoire Charles Coulomb (L2C), Université de Montpellier, CNRS, Montpellier FR-34095, France

^{a)} Author to whom correspondence should be addressed: wilfried.desrat@umontpellier.fr

ABSTRACT

We report on the growth of 2D layered indium selenide films on (0001)-oriented sapphire substrates by coevaporation. The $\theta - 2\theta$ x-ray diffractograms reveal that the (00 l) planes are preferentially oriented parallel to the substrate with a tendency to deviate from the 2D stacking as a function of the growth time. The ϕ -scans performed for the (107) and (1010) orientations of the hexagonal (h) and rhombohedral (r) phases, respectively, reveal that both polytypes coexist in the epitaxial films. We show that the merging of the h-(100), r-(101), h-(101), and r-(102) lines results in different spectral shapes in the $\theta - 2\theta$ scans according to samples, which gives qualitative information about the contribution of each polytype.

© 2022 Author(s). All article content, except where otherwise noted, is licensed under a Creative Commons Attribution (CC BY) license (<http://creativecommons.org/licenses/by/4.0/>). <https://doi.org/10.1063/5.0091675>

I. INTRODUCTION

In the last decade, monochalcogenides (such as GaSe and InSe), which are 2D materials, have established themselves as key components of the next generation of semiconductor devices due to their exceptional tunable electronic properties.^{1–3} One of the major degrees of freedom of these layered structures is the number of stacked sheets. Many remarkable effects have been reported for monolayers, bilayers, or stackings of a few atomic sheets. In indium selenide, the material with which this work is concerned, it has been demonstrated that the number of atomic layers acts on the size and the nature of the bandgap,^{4–7} on the exciton binding energy,⁸ or on the spin-orbit coupling strength.⁹ The stacking layout becomes essential in multilayer systems, where the position of the atoms in a plane relative to the coordinates of the atoms in the neighbor sheets leads to drastic changes in the structure symmetries. In addition, the polymorphism in monolayers,¹⁰ the twist of atomic sheets in bilayer structures,^{11,12} and the polytypism in bulk crystals are some examples of the variety of phenomena that occur in stacked structures. The presence of several polytypes within a device leads inevitably to structural defects that are detrimental to its optical and electronic specifications. Consequently, the correct determination of the polytypism in a 2D layered sample is an elemental identification.

The most efficient tool for probing the crystalline structure of a solid compound is x-ray diffraction (XRD). The common technique performed on epitaxial films and bulk 2D layered materials is the $\theta - 2\theta$ configuration setup. The obtained spectra display the periodic series of well-defined (00 l) peaks, which is often considered as a piece of evidence of the quality of the crystal since it reflects the regular stacking of the 2D atomic planes. The determination of the polytype in this case, unlike in powders, is subtle since several stacking orders may have very close values of the interplanar distance, which is the most relevant lattice parameter in this geometry. For instance, indium selenide is known to crystallize in the following polytypes among others: β -2H ($P6_3/mmc$) with $c = 16.64\text{\AA}$,¹³ ε -2H ($P6m2$) with $c = 16.70\text{\AA}$,¹⁴ and γ -3R ($R3m$) with $c = 24.946\text{\AA}$ (i.e., 16.63\AA for 2 layers).¹⁵ The likeness of the c -lattice parameter for all these phases makes the distinction of each crystalline stacking order from conventional $\theta - 2\theta$ XRD spectra particularly difficult. Furthermore, the simultaneous presence of both polytypes in a sample results in a strong overlap of the XRD lines of each contribution. Consequently, such a simple diffraction pattern may not be, in general, a relevant indicator of the amount of polytypism. Obviously, the weak interlayer bonds along the c -axis of van der Waals 2D layered compounds favor the formation of stacking faults and allow the coexistence of polytypes within the same sample.¹⁶ In Ref. 17, two

polytypes were shown to be stacked one upon the other. However, depending on the growth conditions, the synthesis of 2D materials can also result in single crystals embedded in a matrix of a distinct polytype.¹⁸

In the case of InSe, the formation energy of several polymorphs has been calculated within the framework of the density functional theory.^{19,20} Srouf *et al.* reported that the γ and ϵ polymorphs have the lowest energy and are the most stable phases although the β polytype presents a slightly higher energy and volume per atom.²¹ Nevertheless, the differences between all these crystalline structures are tenuous and do not take the thermodynamic or kinetic mechanisms, which control the bulk or 2D material growth processes into consideration.

In this study, we present the x-ray diffractograms of indium selenide films deposited on *c*-axis oriented sapphire substrates under different growth conditions. We show that all the layers present a good crystalline quality, with a strong preferential orientation. The (00 l) planes are parallel to the surface of the substrate, which is extremely promising for future large scale InSe-based devices. However, a thorough investigation of the XRD data reveals (i) the presence of misoriented crystallites that become more significant as the InSe film becomes thicker and (ii) the coexistence of various amounts of hexagonal and rhombohedral polytypes in all our samples and in commercial bulk InSe, which underlines the difficulty of selecting single phase 2D van der Waals materials. Then, we demonstrate that the relative contribution of the (100) and (101) lines of the hexagonal phase and the (101) and (102) lines of the rhombohedral one gives rise to distinct spectral shapes, depending on the contribution of each phase.

II. GROWTH OF INDIUM SELENIDE FILMS

In this work, we carry out the careful x-ray diffraction analysis of three indium selenide films grown on (0001)-oriented sapphire wafers by coevaporation. These three samples are selected from their representativeness among a batch of several films. Additional data are presented in the [supplementary material](#) for completeness. The wafers are initially soldered with indium on a molybdenum substrate

holder, ensuring a perfect control and homogeneity on the growth temperature, which is fixed at $T_{\text{growth}} = 450^\circ\text{C}$. The pure In and Se elements (5N) are evaporated from Knudsen effusion cells, with a constant indium flux set by a cell temperature of $T_{\text{In}} = 790^\circ\text{C}$. The chamber pressure equals $\sim 10^{-6}$ Torr during the growth. The difference between all three sample resides in the supply of selenium during the growth and the growth duration. The InSe films labeled Nos. 1 and 3 have been deposited with $T_{\text{Se}} = 189^\circ\text{C}$ during 0.5 and 2 h, respectively, while sample No.2 was grown with a lower selenium partial pressure ($T_{\text{Se}} = 185^\circ\text{C}$) during 1 h.

The $\theta - 2\theta$ x-ray diffraction scans of the three InSe films labeled Nos. 1–3 are plotted in Fig. 1(a). The main peaks observed at this scale follow the perfect (00 l) series, which demonstrates the preferential stacking of the InSe planes parallel to the surface of the substrate. The layered macroscopic nature of our layers is confirmed by the atomic force microscopy images of peeled samples (see the [supplementary material](#)). From this plot, it is impossible to discriminate between the contributions of the 3R γ -InSe polytype and the 2H β - or ϵ -InSe phase since the signatures of the stacked planes are almost identical. For the hexagonal InSe, the l indices are even ($l = 2, 4, 6, \dots$), while in the rhombohedral phase, they are replaced by multiples of 3 ($l = 3, 6, 9, \dots$), in agreement with the unit cells sketched in Fig. 1(c). We stress that the XRD spectra of our epitaxial films are qualitatively identical to what is measured on a piece of commercial bulk InSe (topmost curve in Fig. 1). The lower XRD intensity measured in the films mainly relates to the thinner thickness, which is confirmed by the detection of the bottom sapphire substrate. The growth rate has been evaluated as ~ 10 nm/min, leading to the film thicknesses of 300, 600, and 1200 nm for sample Nos. 1–3, respectively.

III. DETERMINATION OF THE HEXAGONAL AND RHOMBOHEDRAL POLYTYPES BY X-RAY DIFFRACTION

In order to determine the polytypes of the grown films, we performed ϕ -scans after locking on one selected peak with an out-of-*c*-axis orientation, namely, the (107) and (1010) crystallographic

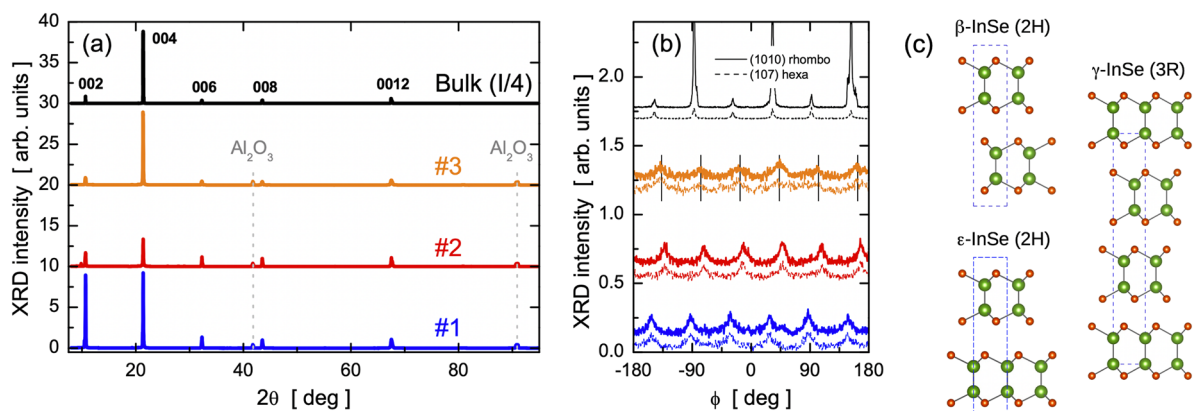


FIG. 1. (a) $\theta - 2\theta$ XRD scans of bulk and three InSe films (Nos. 1–3) grown by epitaxy on (0001)-sapphire substrates. Gray vertical dashed lines indicate the peaks arising from sapphire. (b) ϕ -scans performed on the (1010) and (107) peaks in the rhombohedral and hexagonal polytypes, respectively. Thin vertical lines indicate a 60° periodicity. (c) Side view of the unit cells of hexagonal β - and ϵ -InSe and rhombohedral γ -InSe.

planes for the hexagonal and rhombohedral InSe, respectively. The curves plotted in Fig. 1(b) reveal that all three samples contain both the hexagonal and rhombohedral polytypes with a preferential in-plane orientation. The common phase of the ϕ -scan oscillations shows that the in-plane orientations of the 2H and 3R phases are linked. Note that the rhombohedral polytype exhibits a 60° periodicity highlighted by the thin vertical lines in Fig. 1(b) instead of the 120° expected one. It is attributed to the contributions of different r-InSe layers twisted by 60° . The background signal and the width of the peaks agree with significant misorientations and a lower in-plane crystal quality than along the growth axis.

Figure 2 presents the XRD traces of the same three samples in a smaller intensity range that permits the showing of much weaker structures (the approximative magnification factor equals 160). No additional significant feature except for the attenuated K_β and tungsten replicas of the main InSe and sapphire peaks of the (00l) series can be observed in the lowest scan (sample No.1) of this figure. These peaks, indicated by the diamond symbols in the lowest curve of Fig. 2, result from the use of a Göbel mirror in the primary x-ray beam path to enhance the detectivity. The two other spectra show extra diffraction lines. The spectrum of sample No.2 consists of a large number of peaks that are attributed for most of them to the polycrystalline In_4Se_3 phase and are indexed with star symbols in Fig. 2. It is consistent with the lower temperature of the selenium cell, 185°C instead of 189°C for sample No.1, which favors the growth of the selenium sub-stoichiometric phase, i.e., In_4Se_3 . The unit cell of this compound is orthorhombic with the $Pnmm$ space group,^{22–24} which results in a large number of nonequivalent diffracting planes. The main XRD peak of this compound occurs at $2\theta = 28.95^\circ$ for the (131) orientation. Here, this peak is the most intense of the In_4Se_3 diffractogram, but it remains 200 times smaller than the main (004) peak of InSe, which is the major phase.

Now, focusing on the $[25^\circ\text{--}27^\circ]$ 2θ range highlighted by the dashed rectangle in Fig. 2, we notice the existence of two peaks slightly broader than the adjacent ones. The In_4Se_3 phase cannot account for this observation. Interestingly, this two-peak structure

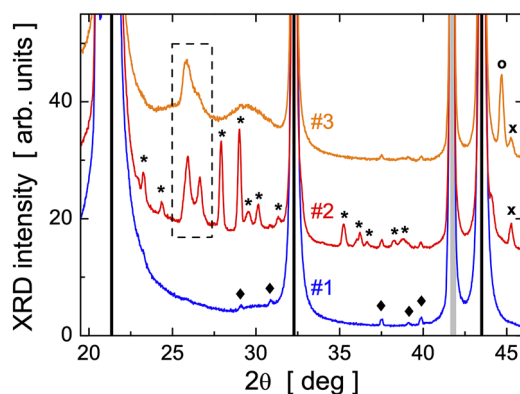


FIG. 2. X-ray diffraction spectra of the three InSe films preferentially oriented along the c -axis. The thick solid vertical lines indicate the (00l) peaks. The diamonds indicate the K_β and tungsten replicas of the main peaks, and the stars indicate the peaks attributed to the In_4Se_3 phase. The dashed rectangle delimits the part enlarged in Fig. 3.

takes a different shape in sample No.3 with a strongly asymmetric shape. Finally, we underline that two narrow peaks are also detected at 44.70° and 45.25° , which are indicated by the circle and cross-mark symbols, respectively, in Fig. 2. The latter is observed in sample No.2 as well, and it is attributed to the (110) planes shared by the hexagonal and rhombohedral phases (see the last row in Table I).

The $\theta - 2\theta$ diffractograms of sample Nos. 2 and 3, recorded over a long acquisition time, are plotted in Fig. 3. The 2θ span corresponds to the dashed rectangle area in Fig. 2, i.e., it ranges between 25° and 27.25° . The vertical dashed lines indicate the position of the diffracted lines of the hexagonal and rhombohedral polymorphs of InSe and In_4Se_3 phases. For InSe, the 2θ values are taken from the 034-1431 and 042-0919 powder diffraction files, respectively, and are reported in Table I with their relative intensities and hkl indices. The diffraction angles given for the hexagonal β polytype are identical for the ϵ stacking. From the XRD analysis alone, we are not able to discriminate between both structures. However, the detection of the photoluminescence (PL) in our InSe films, presented in the supplementary material, is in favor of the β polytype. Indeed, the ϵ phase has an indirect bandgap,²⁵ and as a consequence, the PL must be quenched by the nonradiative emission that dominates the radiative one. From Fig. 3, it is obvious that the two peaks observed in sample No.2 correspond to the (101) and (102) planes of the rhombohedral crystalline phase, named r101 and r102. A two-peak fit of the experimental diffraction spectrum using a Gaussian broadening (thin blue line) is, however, insufficient to reproduce correctly the data. Taking into account the two interlaid contributions of the hexagonal phase, namely, the (100) and (101) lines, allows us to fit the x-ray diffractogram satisfactorily (black solid line). The long tail that occurs for $2\theta > 26.8^\circ$ mainly results from the non-zero background induced by the neighbor In_4Se_3 peak at 27.91° (see Fig. 2). The In_4Se_3 lines at 25.78° (211) and 26.86° (121) seem to play a

TABLE I. 2θ , intensity, and hkl indices of the diffraction peaks of the hexagonal and rhombohedral InSe phases limited to the $[20^\circ\text{--}46^\circ]$ 2θ range. The data are extracted from the study by Popović *et al.* ($a = 4.005 \text{ \AA}$ and $c = 16.64 \text{ \AA}$)²⁶ and Rigoult *et al.* ($a = 4.002 \text{ \AA}$ and $c = 24.946 \text{ \AA}$).¹⁵ For the rhombohedral phase, the hexagonal-like indices are used (i.e., 006 instead of 222). The different cell parameters obtained in both refinements lead to a slight discrepancy in the 2θ values for the common diffraction conditions.

Hexagonal InSe			Rhombohedral InSe		
2θ	Intensity	hkl	2θ	Intensity	hkl
21.29°	100	004	21.35°	72	006
25.69°	2	100	25.93°	100	101
26.11°	3	101	26.67°	68	102
30.38°	2	103	31.40°	30	105
32.25°	10	006	32.27°	4	009
37.44°	3	105	36.12°	34	107
43.47°	8	008	38.81°	67	108
45.30°	4	110	43.50°	4	0012
			45.28°	82	110

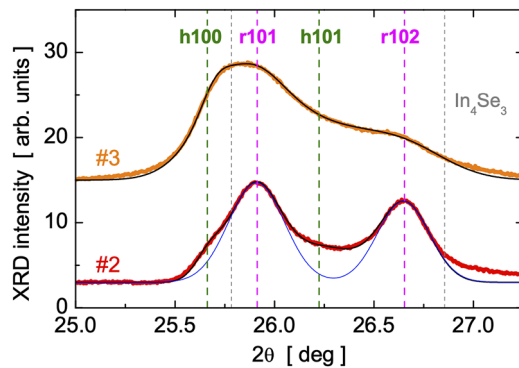


FIG. 3. Main graph: slow $\theta - 2\theta$ diffraction scans of the InSe films (Nos. 2 and 3) with multi-peak fitting (blue and black solid lines). The dashed vertical lines indicate the position of the expected diffraction lines for the hexagonal InSe, rhombohedral InSe, and In_4Se_3 compounds (green, pink, and gray lines, respectively).

negligible role in the overall spectral shape in this 2θ range. This is even more true for the fit of the diffractogram of sample No.3, where no trace of In_4Se_3 was detected in this film. The asymmetric shape in the case of sample No.3 can also be fitted with four Gaussian-broadened peaks. The fitting parameters of the peaks of the hexagonal phase are almost the same as for sample No.2, but those for the rhombohedral InSe peaks that govern the overall shape have to be changed. The ratio of the (101)/(102) peak magnitudes increases from 1.2 for sample No.2 to 2.6 for sample No.3, the peak broadening is enlarged by 60%, and the peak positions are downshifted by $\sim 0.04^\circ$.

IV. X-RAY DIFFRACTOGRAMS OF InSe POWDERS

The patterns observed in the x-ray diffraction spectra of sample Nos. 2 and 3 around $2\theta \approx 26^\circ$ result from the atomic planes of rhombohedral and hexagonal InSe, which are not parallel to the substrate, i.e., (10 l)-oriented planes. From Table I, it is not surprising to observe the peaks associated with the rhombohedral polymorph since their relative intensities are very large with 100% and 68% for the (101) and (102) lines, respectively. At the opposite, the relative intensities of the (100) and (101) peaks of the hexagonal phase are weak, less, or equal to 3%. Nevertheless, the intensity values determined from powder diffractograms cannot account for the peak intensities in strongly c -axis oriented epitaxial InSe films. A proof of this resides in the detection of a noticeable peak at 44.70° reported previously in sample No.3, which does not appear in the standard powder diffraction file because of its smallness (see Table I). In fact, this 2θ value corresponds to the (1011) plane of r-InSe.

With the aim of estimating the relative amount of the hexagonal and rhombohedral polytypes, we performed $\theta - 2\theta$ scans on the films reduced to powder beforehand. They are plotted in Fig. 4(b) along with the diffractograms of the as-grown layers for comparison. For sample No.1, the diffraction peaks linked to the (10 l)-oriented planes appear in the powder, while they were not detected in the epitaxial film. The maximum peak lies in the vicinity of the h-(101) line, which suggests a relatively high amount of the hexagonal polytype in

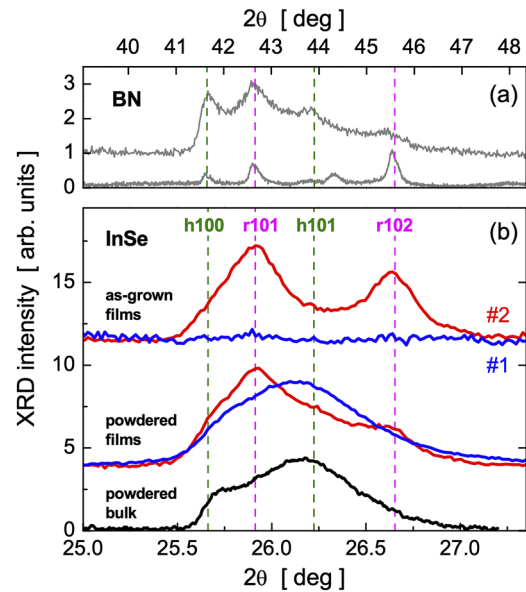


FIG. 4. (a) X-ray diffractograms of turbostratic (top) and graphitic (bottom) boron nitride samples. (b) X-ray diffractograms of as-grown (top) and reduced to powder (center) InSe films (Nos. 1 and 2). The bottom trace is measured from powdered bulk InSe.

this sample as compared to sample No.2. Indeed, the two-peak shape of the as-grown No.2 film transforms into a more asymmetric form while keeping pronounced rhombohedral contributions. This analysis remains qualitative, but it demonstrates that the spectral shape in this 2θ region gives valuable information on the polytypism present in a sample. This way, we find out that a piece of commercial bulk “ γ -InSe” contains both hexagonal and rhombohedral polytypes as well. It is further confirmed by the series of ϕ scans plotted in Fig. 2(b).

V. DISCUSSION

The InSe films presented in this study have a thickness spreading from 0.3 to 1.2 μm , and as a consequence, the x-rays probe the samples in their entirety down to the sapphire substrate. Thus, we can establish that the majority of the films of this study are composed of (00 l) preferentially oriented InSe crystallites with their normal parallel to the c -axis of Al_2O_3 . Sample No.1, which is grown with the same conditions as sample No.3 but during half an hour instead of 2 h, shows the (00 l) diffraction lines only, suggesting a perfect 2D stacking with an inappreciable quantity of misoriented crystallites. As the film thickness increases, the formation of crystallites with other crystalline orientations occurs. The XRD analysis demonstrates, however, that the orientation of the detected planes remains not too far from the (00 l) direction, like r-(1011) detected at 44.70° . The detection of the hexagonal and rhombohedral polytypes indicates that both phases form during the growth from their initial stage in all samples. The in-plane lattice constants are extremely close for both polytypes, which facilitates the creation of the 2H and 3R stackings. The lower partial pressure of selenium in sample No.2

tends to favor the formation of the latter, but the influence of the coexisting In_4Se_3 phase cannot be ruled out.

It is interesting to compare the data measured in our InSe films with the diffractograms of other 2D compounds, which also show polytypism. Thus, we present the $\theta - 2\theta$ scans of two boron nitride samples in Fig. 4(a) by following the work of Yuan *et al.*²⁷ We present the XRD spectra of one commercial BN powder and one Bernal BN high-quality crystal.¹⁸ The rescaling of the 2θ axis allows us to match the positions of the h-(100), r-(101), h-(101), and r-(102) lines in the BN and InSe materials. The peaks are well distinct in the case of graphitic BN [lowest spectrum in Fig. 4(a)]. In turbostratic BN, the (10l) peaks are known to merge in a broad asymmetric (10) line with a long tail on the high 2θ angle side.^{28–30} In addition, the increased interplanar distance in the turbostratic material translates into a slight downshift and broadening of the 2θ diffraction angles with respect to the line positions in the ideal graphitic structure. There is, however, no similar feature in our InSe films that could suggest a disordered turbostratic growth on top of the effects of the crystallite size, microstrain, and stacking disorder in our polycrystalline and polymorphic InSe films.

VI. CONCLUSION

Indium selenide films have been grown on *c*-plane sapphire wafers by van der Waals epitaxy. We show that the 2D crystallites are (00l) oriented, predominantly parallel to the substrate in thin films, while misoriented planes appear when the film thickness increases. However, this issue will be of minimum consequence for the crystalline growth of ultra-thin InSe layers. The coexistence of the hexagonal and rhombohedral polytypes in our samples is demonstrated by x-ray diffraction ϕ -scans performed for out-of-*c*-axis orientation planes. However, the detection of the (10l) diffraction peaks in the more common $\theta - 2\theta$ configuration between 25° and 27° allows a fast qualitative estimation of the contributions of the hexagonal and rhombohedral polytypes. Finally, we did not report the observation of turbostratic stacking in our InSe films.

SUPPLEMENTARY MATERIAL

See the [supplementary material](#) for additional x-ray diffractograms of InSe layers grown with different experimental conditions, low temperature photoluminescence spectra, and an atomic force microscopy image of a peeled InSe thin film.

AUTHOR DECLARATIONS

Conflict of Interest

The authors have no conflicts to disclose.

DATA AVAILABILITY

The data that support the findings of this study are available from the corresponding author upon reasonable request.

REFERENCES

- H. Cai, Y. Gu, Y.-C. Lin, Y. Yu, D. B. Geohegan, and K. Xiao, "Synthesis and emerging properties of 2D layered III–VI metal chalcogenides," *Appl. Phys. Rev.* **6**, 041312 (2019).
- Z. Yang and J. Hao, "Recent progress in 2D layered III–VI semiconductors and their heterostructures for optoelectronic device applications," *Adv. Mater. Technol.* **4**, 1900108 (2019).
- K. Khan, A. K. Tareen, M. Aslam, R. Wang, Y. Zhang, A. Mahmood, Z. Ouyang, H. Zhang, and Z. Guo, "Recent developments in emerging two-dimensional materials and their applications," *J. Mater. Chem. C* **8**, 387–440 (2020).
- G. W. Mudd, M. R. Molas, X. Chen, V. Zolyomi, K. Nogajewski, Z. R. Kudrynskiy, Z. D. Kovalyuk, G. Yusa, O. Makarovskiy, L. Eaves, M. Potemski, V. I. Fal'ko, and A. Patané, "The direct-to-indirect band gap crossover in two-dimensional van der Waals indium selenide crystals," *Sci. Rep.* **6**, 39619 (2016).
- D. A. Bandurin, A. V. Tyurnina, G. L. Yu, A. Mishchenko, V. Zolyomi, S. V. Morozov, R. K. Kumar, R. V. Gorbachev, Z. R. Kudrynskiy, S. Pezzini, Z. D. Kovalyuk, U. Zeitler, K. S. Novoselov, A. Patané, L. Eaves, I. V. Grigorieva, V. I. Fal'ko, A. K. Geim, and Y. Cao, "High electron mobility, quantum Hall effect and anomalous optical response in atomically thin InSe," *Nat. Nanotechnol.* **12**, 223–227 (2017).
- H. Henck, D. Pierucci, J. Zribi, F. Bisti, E. Papalazarou, J.-C. Girard, J. Chaste, F. m. c. Bertran, P. Le Fèvre, F. Sirotti, L. Perfetti, C. Giorgetti, A. Shukla, J. E. Rault, and A. Ouerghi, "Evidence of direct electronic band gap in two-dimensional van der Waals indium selenide crystals," *Phys. Rev. Mater.* **3**, 034004 (2019).
- C. Song, S. Huang, C. Wang, J. Luo, and H. Yan, "The optical properties of few-layer InSe," *J. Appl. Phys.* **128**, 060901 (2020).
- J. Zultak, S. J. Magorrian, M. Koperski, A. Garner, M. J. Hamer, E. Tóvári, K. S. Novoselov, A. A. Zhukov, Y. Zou, N. R. Wilson, S. J. Haigh, A. V. Kretinin, V. I. Fal'ko, and R. Gorbachev, "Ultra-thin van der Waals crystals as semiconductor quantum wells," *Nat. Commun.* **11**, 125 (2020).
- A. Ceferino, S. J. Magorrian, V. Zolyomi, D. A. Bandurin, A. K. Geim, A. Patané, Z. D. Kovalyuk, Z. R. Kudrynskiy, I. V. Grigorieva, and V. I. Fal'ko, "Tunable spin-orbit coupling in two-dimensional InSe," *Phys. Rev. B* **104**, 125432 (2021).
- H. Bergeron, D. Lebedev, and M. C. Hersam, "Polymorphism in post-dichalcogenide two-dimensional materials," *Chem. Rev.* **121**, 2713–2775 (2021).
- Q. Xu, Y. Guo, and L. Xian, "Moiré flat bands in twisted 2D hexagonal vdW materials," *2D Mater.* **9**, 014005 (2022).
- X. Yao and X. Zhang, "Electronic structures of twisted bilayer InSe/InSe and heterobilayer graphene/InSe," *ACS Omega* **6**, 13426–13432 (2021).
- B. Čelustka and S. Popović, "The synthesis of In_2Se_6 and In_2Se from InSe by zone-melting process," *J. Phys. Chem. Solids* **35**, 287–289 (1974).
- A. Chevy, "Growth of indium selenides by vapour phase chemical transport; polytypism of indium monoselenide," *J. Cryst. Growth* **51**, 157–163 (1981).
- J. Rigoult, A. Rimsky, and A. Kuhn, "Refinement of the 3R γ -indium monoselenide structure type," *Acta Crystallogr., Sect. B* **36**, 916–918 (1980).
- C. De Blasi, D. Manno, and A. Rizzo, "Study of the polytypism in melt grown InSe single crystals by convergent beam electron diffraction," *J. Cryst. Growth* **100**, 347–353 (1990).
- C. De Blasi, D. Manno, S. Mongelli, and A. Rizzo, "Electron diffraction study of melt-grown InSe crystals," *Nuovo Cimento D* **7**, 795–806 (1986).
- A. Rousseau, M. Moret, P. Valvin, W. Desrat, J. Li, E. Janzen, L. Xue, J. H. Edgar, G. Cassabois, and B. Gil, "Determination of the optical bandgap of the Bernal and rhombohedral boron nitride polymorphs," *Phys. Rev. Mater.* **5**, 064602 (2021).
- L. Ghalouci, F. Taibi, F. Ghalouci, and M. O. Bensaid, "Ab initio investigation into structural, mechanical and electronic properties of low pressure, high pressure and high pressure-high temperature phases of indium selenide," *Comput. Mater. Sci.* **124**, 62–77 (2016).
- J. Srouf, M. Badawi, F. El Haj Hassan, and A. Postnikov, "Comparative study of structural and electronic properties of GaSe and InSe polytypes," *J. Chem. Phys.* **149**, 054106 (2018).
- J. Srouf, A. Postnikov, M. Badawi, and F. El Haj Hassan, "Competing structures in (In,Ga)Se and (In,Ga)₂Se₃ semiconductors," *Phys. Status Solidi B* **254**, 1700120 (2017).

- ²²A. Likforman and J. Etienne, "Structure cristalline de In_4Se_3 ," *C. R. Acad. Sc. Paris, Série C* **275**, 1097–1100 (1973).
- ²³J. H. C. Hogg, H. H. Sutherland, and D. J. Williams, "The crystal structure of tetraindium triselenide," *Acta Crystallogr., Sect. B* **29**, 1590–1593 (1973).
- ²⁴U. Schwarz, H. Hillebrecht, H. Deiseroth, and R. Walther, " In_4Te_3 und In_4Se_3 : Neubestimmung der kristallstrukturen, druckabhängiges verhalten und eine bemerkung zur nichtexistenz von In_4S_3 ," *Z. Kristallogr. - Cryst. Mater.* **210**, 342–347 (1995).
- ²⁵A. Politano, D. Campi, M. Cattelan, I. Ben Amara, S. Jaziri, A. Mazzotti, A. Barinov, B. Gürbulak, S. Duman, S. Agnoli, L. S. Caputi, G. Granozzi, and A. Cupolillo, "Indium selenide: An insight into electronic band structure and surface excitations," *Sci. Rep.* **7**, 3445 (2017).
- ²⁶S. Popović, A. Tonejc, B. Čelustka, B. Gržeta-Plenković, and R. Trojko, "Revised and new crystal data for indium selenides," *J. Appl. Crystallogr.* **12**, 416–420 (1979).
- ²⁷S. Yuan, C. Journet, S. Linas, V. Garnier, P. Steyer, S. Benayoun, A. Brioude, and B. Toury, "How to increase the h-BN crystallinity of microfilms and self-standing nanosheets: A review of the different strategies using the PDCs route," *Crystals* **6**, 55 (2016).
- ²⁸M.-G. Balint and M. Petrescu, "Crystallographic features of hBN as a precursor in the cBN high-temperature-high-pressure synthesis," *U.P.B. Sci. Bull., Series B* **69**, 79–90 (2007).
- ²⁹M. Chubarov, H. Pedersen, H. Högberg, J. Jensen, and A. Henry, "Growth of high quality epitaxial rhombohedral boron nitride," *Cryst. Growth Des.* **12**, 3215–3220 (2012).
- ³⁰M. Moret, A. Rousseau, P. Valvin, S. Sharma, L. Souqui, H. Pedersen, H. Högberg, G. Cassabois, J. Li, J. H. Edgar, and B. Gil, "Rhombohedral and turbostratic boron nitride: X-ray diffraction and photoluminescence signatures," *Appl. Phys. Lett.* **119**, 262102 (2021).